

OTOLITH ULTRASTRUCTURE OF SMOOTH OREO, *PSEUDOCYTTUS MACULATUS*, AND BLACK OREO, *ALLOCYTTUS* SP., SPECIES

N. M. DAVIES,¹ R. W. GAULDIE,^{1,2} S. A. CRANE,¹ AND
R. K. THOMPSON³

ABSTRACT

The ultrastructure of sagittal otoliths from 14 *Pseudocyttus maculatus* and 25 *Allocyttus* sp. individuals were examined to determine their suitability for estimating age in these two species. Scanning electron microscopy revealed high levels of complexity in both external surface topography and internal structural organization in the sagittae of both species. Many different crystal forms were found, including calcite-like prisms. A close similarity in otolith structure exists between the two species. Deposition of check rings analogous to annual and daily growth increments was found to be irregular with the underlying complexity of crystalline growth obscuring the finer (analogous to daily) growth rings, making their periodicity difficult to validate and implying that with present techniques the sagittal otoliths of the oreo species *Pseudocyttus maculatus* and *Allocyttus* sp. are not suitable for age estimation.

The smooth oreo, *Pseudocyttus maculatus*, and the black oreo, *Allocyttus* sp., are two related species of the family Oreosomatidae. They are both important commercial species in New Zealand. The black oreo is the most commonly caught oreo in New Zealand waters, while the smooth oreo is the second-most commonly caught oreo. Little is known about the biology of these fish. The black oreo is endemic to New Zealand while the smooth oreo occurs in New Zealand, South Australian, South African, and South American waters (Last et al. 1983). In the waters south of New Zealand, the distributions of the two species overlap (McMillan 1985). The habitat range of the smooth oreo is between 650 and 1,200 m, and that of the black oreo is between 600 and 1,200 m (McMillan 1985).

A preliminary examination of the ultrastructure of otoliths [sagittae] of these fish was undertaken as part of a study to establish an ultrastructural basis for a suitable ageing technique. This study describes the external and internal structure and organization of the otoliths in terms of the suitability of the various check rings of the sagittae for age estimation.

MATERIALS AND METHODS

Three otoliths (the sagitta, astericus, and lapillus)

are contained in the endolymphatic sac (Fig. 1a). The sagitta is the largest otolith and is located in the most ventral position in the sac. The arrangement of the three otoliths in the endolymphatic sac ranges between the primitive where a large astericus and sagitta with no lapillus is present (Gauldie et al. 1986) and the typical teleost arrangement where a small astericus is located close to the sagitta, and an even smaller lapillus is displaced into the atrium of the semi-circular canal. The oreosomatids are primitive fishes taxonomically, lying in the order Beryciformes (Nelson 1976), and the arrangement of otoliths reflects the taxonomic position of the fish. The orientation of otoliths described here refers to the orientation in situ. The lateral face is the outward (antisulcal) surface; the medial face is the inward (sulcal) surface. Investigation was restricted to the sagitta primarily because of the difficulties in establishing homologies for daily and annual type check rings in the astericus and lapillus.

Sagittae were dissected from 14 smooth and 25 black oreo individuals caught in bottom trawls off the east coast of New Zealand. These individuals ranged in length from 24.5 to 40.1 cm (black oreo) and 35.1 to 51.2 cm (smooth oreo).

Whole otoliths were photographed at 6× to 20× using a WILD⁴ photomicroscope. The sagittae were embedded on glass slides in epoxy resin with the antisulcus surface uppermost and finely ground on a Struers Planapol-2 petrographic grinder. The

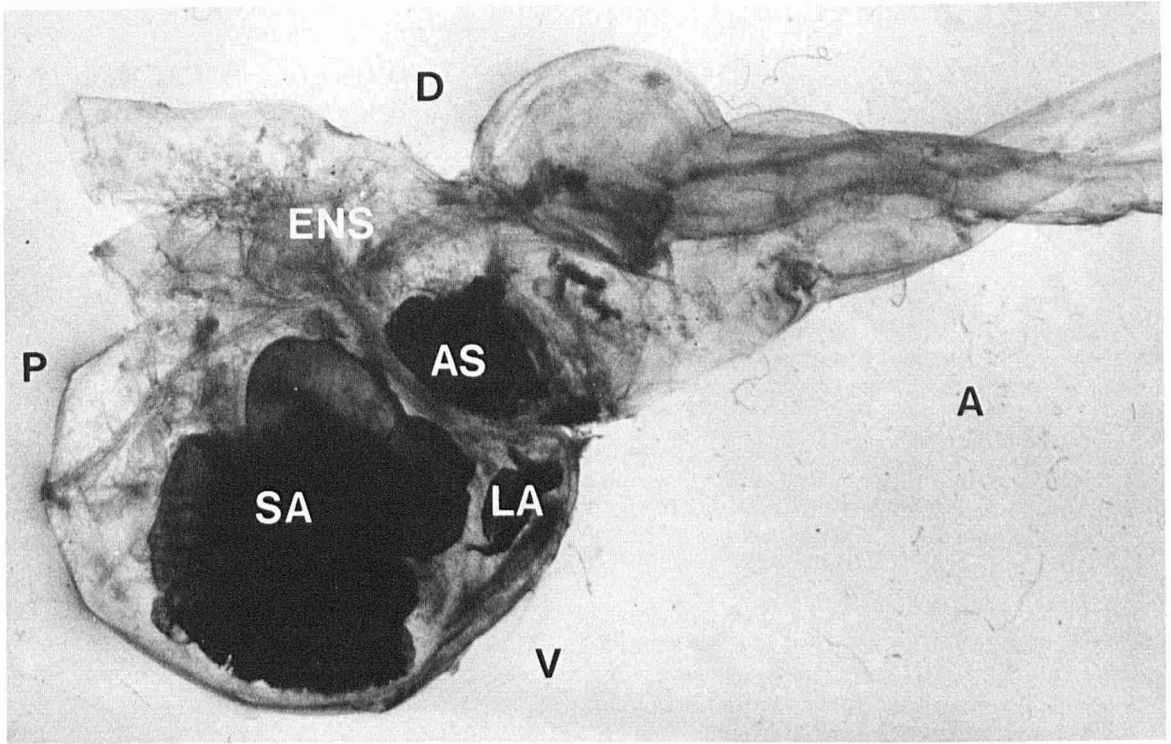
¹Fisheries Research Centre, Ministry of Agriculture and Fisheries, Greta Point, Evans Bay Parade, P.O. Box 297, Wellington, New Zealand.

²To whom reprint requests should be sent.

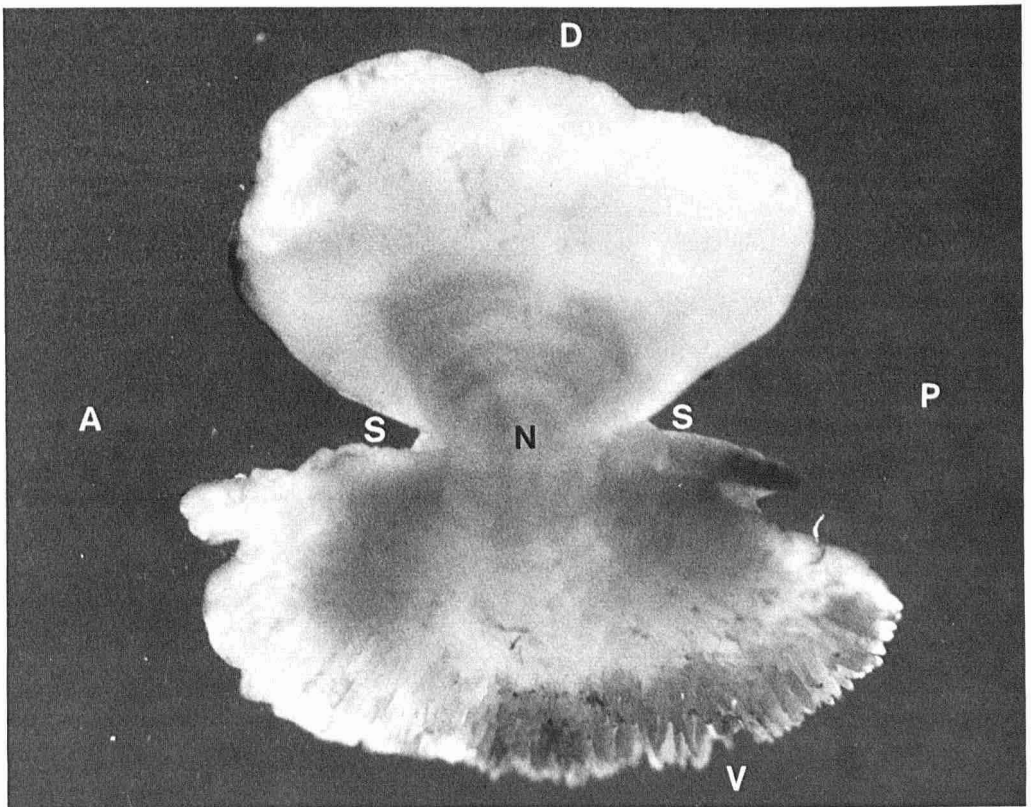
³Electron Microscope Unit, Kirk Building, Victoria University of Wellington, Private Bag, Wellington, New Zealand.

⁴Reference to trade names does not imply endorsement by the National Marine Fisheries Service, NOAA.

a



b



C



FIGURE 1a.—Relative positions of the otoliths in the right endolymphatic sac (ENS) of the smooth oreo in lateral view: astericus (AS), lapillus (LA), and sagitta (SA). Anterior (A), dorsal (D), posterior (P), and ventral (V) surfaces are indicated. Magnification = 6.3 \times .

b.—Dorsal (regular) and ventral (irregular) lobes of the otolith in lateral view, nucleus (N), sulcus (S), and rest as in Figure 1a. Magnification = 12.5 \times .

c.—SEM of the lateral surface topography of the otolith. Scale bar = 1 mm.

ground surface was polished with 2000 grit wet and dry paper to yield a smooth surface for etching. The most successful results were obtained by etching with a 0.1 M solution of disodium salt of EDTA. The otoliths were immersed in this solution for 15 to 20 minutes. Other suitable etching solutions employed were 1) a 1% solution of HCl for 20 to 30 seconds and 2) a 2% solution of Histolab RDO (a commercial etching solution comprising a mixture of HCl and EDTA) for 5 minutes. A cellulose acetate peel was made of the etched surface to obtain an exact replica of the surface features. The peel was placed on a microscope slide under a cover slip, cleared with ethanol or distilled water, viewed, and photographed using a Zeiss photomicroscope. Direct observations

of thin sections (about 20 μ m) of otoliths did not show any more information than that observed in acetate peels. Acetate peels had the advantage of allowing successive grinds to be examined thereby avoiding the problem of losing information that might be located only in very narrow layers within the otolith.

Scanning electron microscope (SEM) photographs were taken of otoliths using a Phillips 505 SEM. Whole otoliths were glued on to SEM pin type mounts, cemented in position with contact cement, and sputter-coated with gold at approximately 5 Torr. The external surface topography of both the medial and lateral faces of the otoliths was photographed. Selected pieces of otoliths broken by thumb

pressure were examined and photographed to obtain internal structural information. Finely ground cross-section surfaces were also polished and etched for examination with the SEM.

RESULTS

Smooth Oreo Otolith

The sagitta is clearly divided into two distinct structures: a small, smooth, regular dorsal lobe and a larger, irregular ventral lobe (Fig. 1b). The irregular lobe has branched crystal formations and clefts at the ventral edge. The lateral face topography is complex (Fig. 1c). The central bumpy area contains the nucleus between the two lobes. Radiating outwards from the nucleus are concentric ridges on the antisolcal surface.

The crystal morphology of the lateral surface of the sagitta is variable. Over much of the central parts of the sagitta, large and variably oriented

crystals give a coarse appearance to the surface of the otolith (Fig. 2a) which presumably obstructs, by diffraction, potentially clear zones in the whole otolith viewed by transmitted light. At the edge of the regular lobe, the crystal type alters to form slabs of crystal layers (Fig. 2b). The analogous area on the irregular lobe yields variable crystalline structures with complex alignments (Fig. 2c). Deep troughs and branching furrows break up the crystal forms at the edge of the irregular lobe.

The medial surface has three distinct parts: the central sulcal area, the edge of the irregular lobe, and the edge of the regular lobe (Fig. 3a). Raised ridges and two prominent knobs are found in the central sulcal area. Crystals compacted into a petal-like growth pattern are found in this part of the otolith (Fig. 3b). Contrasting to this, more porous crystal structures occur in the edge areas of the regular lobe (Fig. 3c). Further variety is found on the irregular lobe, where a very porous, honeycomb-like crystal arrangement exists (Fig. 3d). At the

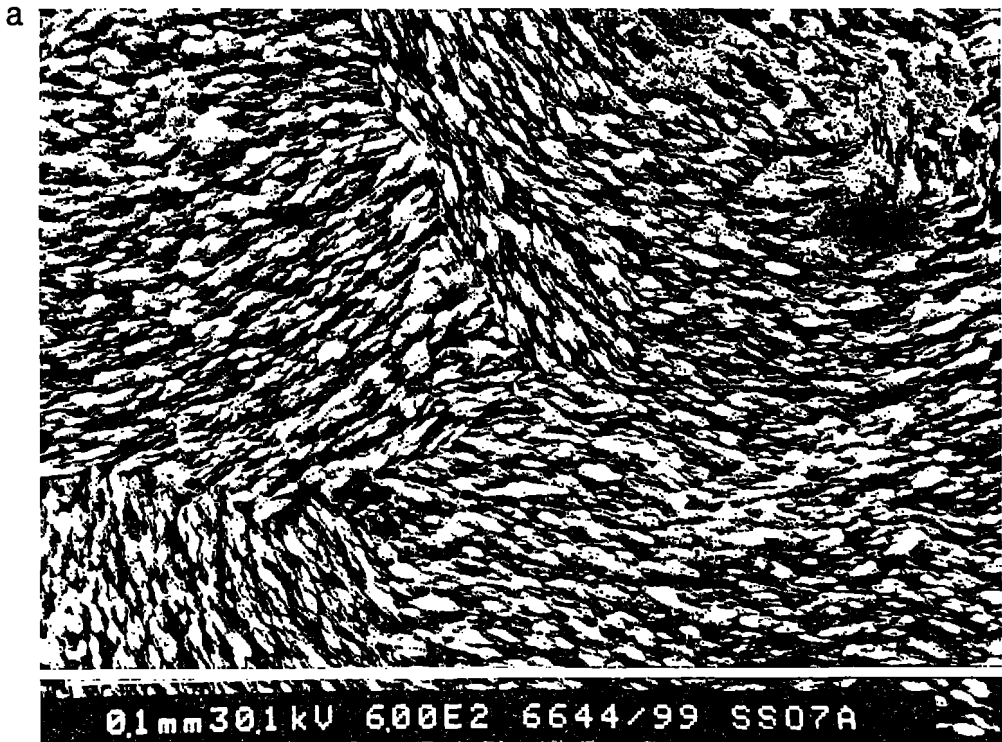
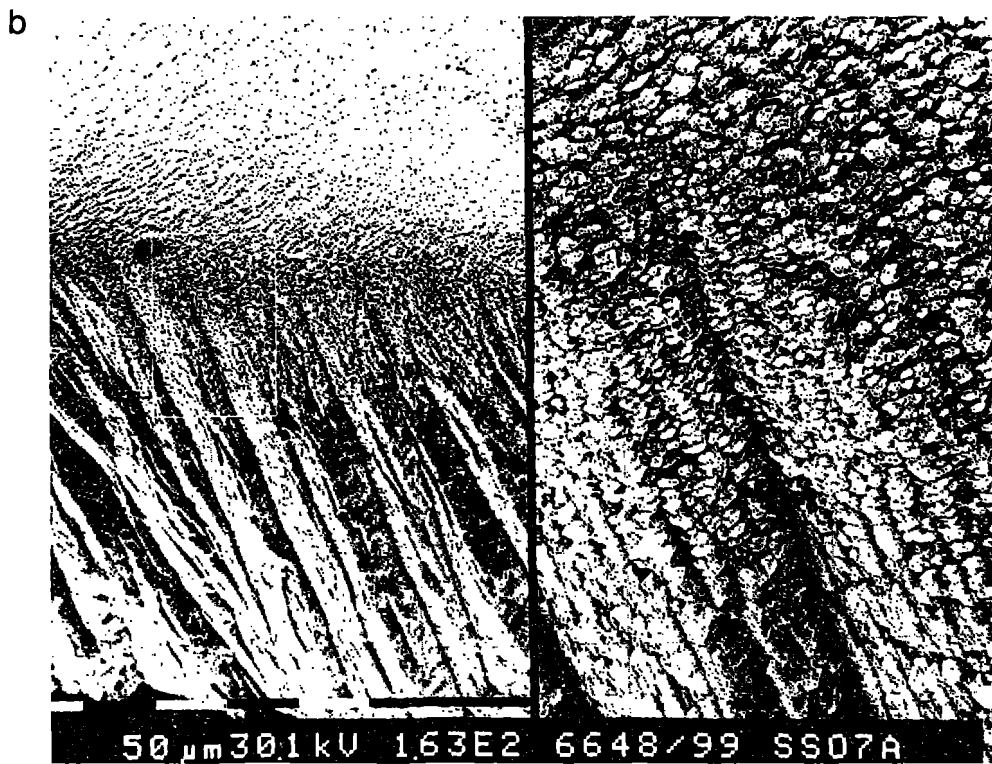


FIGURE 2a.—Coarse crystal structure of the central lateral surface of the smooth oreo otolith. Scale bar = 0.1 mm.
 b.—Split-screen SEM of the transition of the crystal-type at the edge of the lateral surface of the regular lobe. Magnification = 163 \times and 652 \times .
 c.—Haphazard crystal alignments at the edge of the lateral face of the irregular lobe. Scale bar = 0.1 mm.



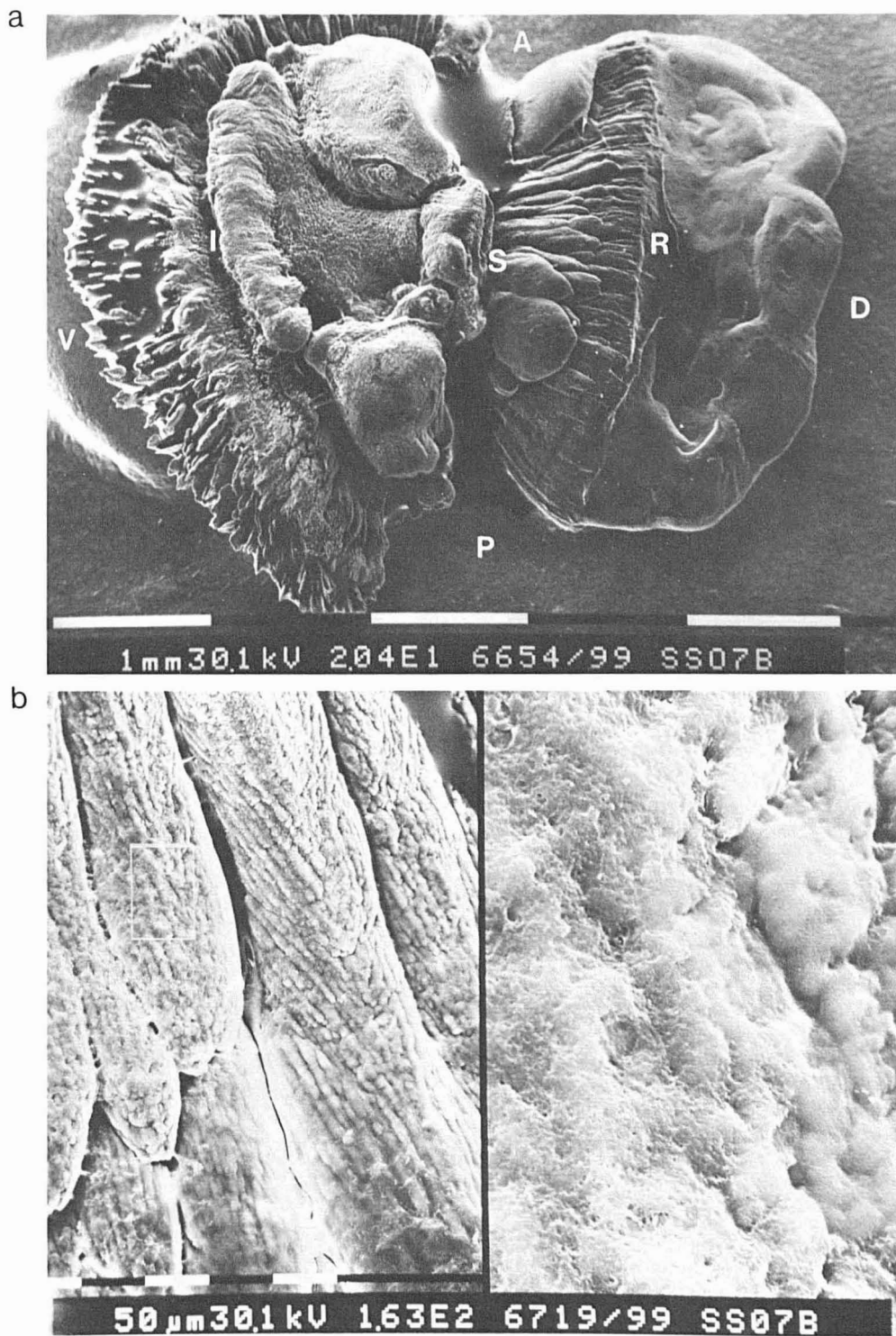


FIGURE 3a.—Medial view of the smooth oreo otolith showing the irregular lobe (I), regular lobe (R), and sulcus (S). Scale bar = 1 mm.

b.—Split-screen SEM of petallike crystal growth in the sulcus on the medial surface. Magnification = 163 \times and 1141 \times .



FIGURE 3c.—Porous crystals on the medial surface of the regular lobe. Scale bar = 10 μ m.

d.—Honeycomblike crystal structure on the medial surface of the irregular lobe. Scale bar = 10 μ m.

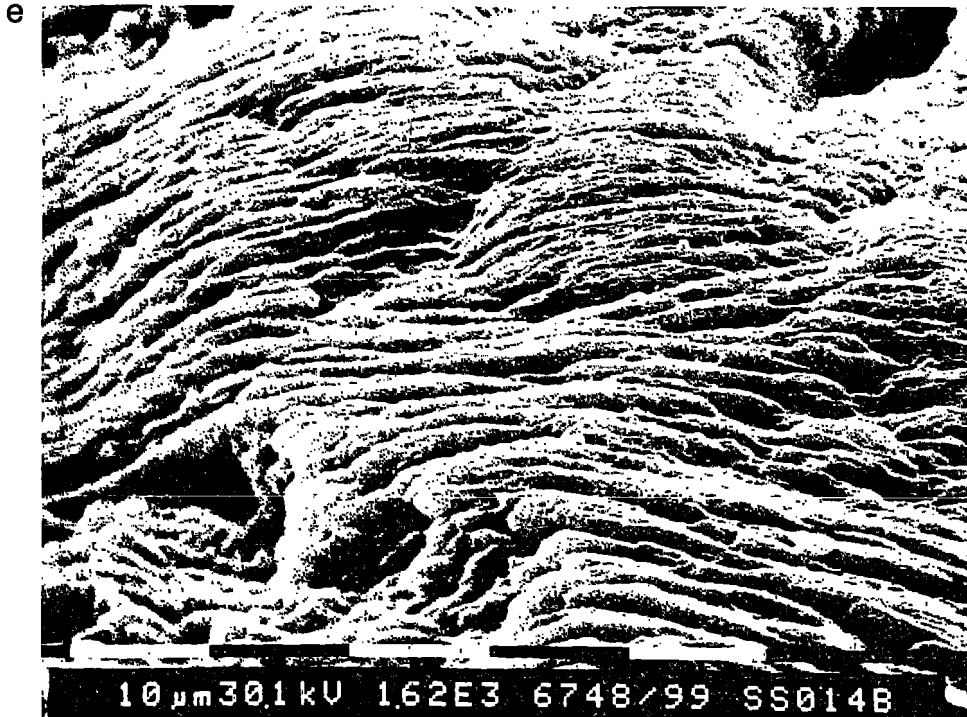


FIGURE 3e.—A laminar pattern of crystalline growth on the medial face of the irregular lobe. Scale bar = 10 μ m.

edge of this lobe, a laminar crystalline growth pattern develops, adding to the overall variation of crystal structures on the medial surface (Fig. 3e). Other studies of otolith ultrastructure present the otolith as homogeneous in crystal form, composed almost entirely of monoclinic aragonite crystals (Degens et al. 1969). The complex crystallinity of the oreo otoliths resembles that of the mollusc shell, which, although aragonitic, often has a pattern of complex variation in crystal habit (Carriker et al. 1980).

Within the broken otolith, the nucleus lies at the center of a spherical primordium (Fig. 4a). Crystals grow outwards from the primordium and epitaxial (Degens 1976) growth patterns exist (Fig. 4b). Complex leaf-shaped crystals occur in areas directly beneath the lateral surface of the fractured irregular lobe (Fig. 4c). Beneath the medial surface, a remarkable series of hexagonal crystals of calcite occur as large rectangular blocks embedded *within* the otolith (Fig. 4d). Calcitic prisms have been described in molluscs as resulting from the regeneration of broken shells (Watabe 1983). It is difficult to imagine otoliths being broken and regenerated in situ.

Major and minor check rings similar to those

described (Gauldie 1987) for otoliths from the orange roughly, a deepwater species from the same habitat, occur (Fig. 4e). When polished and etched, the check rings become clearly visible with deep etched checks occurring between the less deeply etched checks analogous to microscopic growth increments in other species (Fig. 4f). At a higher magnification the finer increments become obscured by the coarseness of the underlying crystal type (Fig. 4g). Those fine increments that are visible occur irregularly and have varying widths.

Large-scale rings analogous to opaque/hyaline annual zones were observed in the regular lobe. The mean width of these zones, measured using transmitted light (Fig. 1b), was 0.34 mm (± 0.06). The concentric ridges observed by SEM on the lateral surface of the regular lobe (Fig. 1c) have a mean width of 0.27 mm (± 0.06). These two structures, opaque/hyaline zones and surface ridges, have about the same width with no statistically significant differences between them.

Examination of otolith cross sections reveals widely spaced, large rings with many finer rings in between (Fig. 4h). When examined in greater detail, the demarcation between the large and finer rings

a

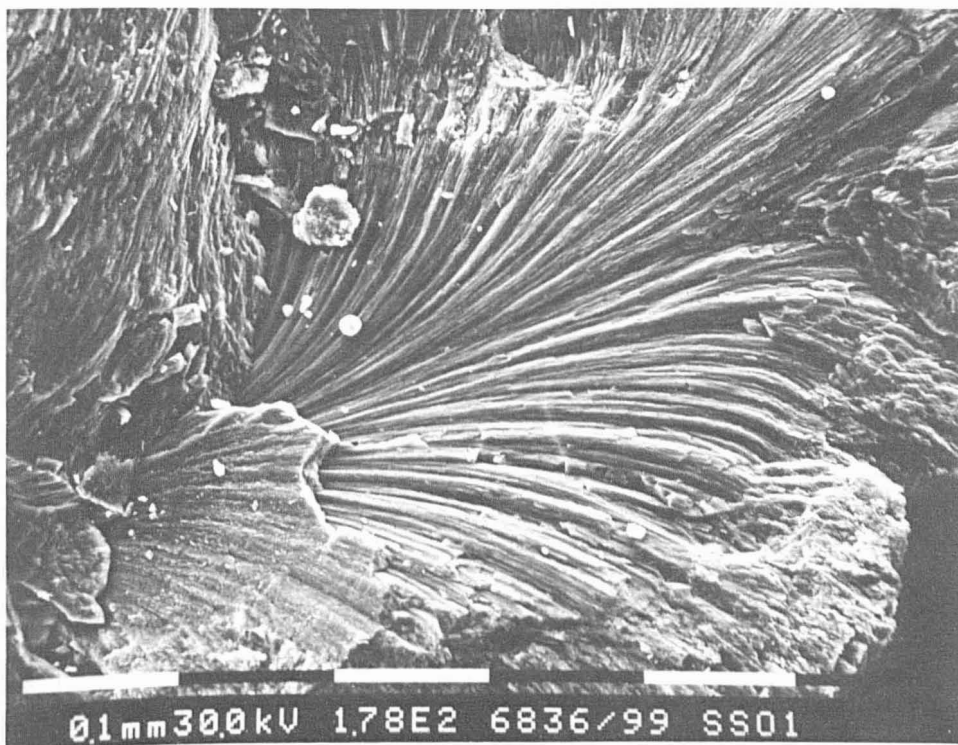


FIGURE 4a.—Broken smooth oreo otolith reveals the spherical primordium (PM) and nucleus (N) and the surrounding radial crystal growth. Scale bar = 0.1 mm.

b.—Epitaxial crystal development in the broken otolith. Scale bar = 0.1 mm.

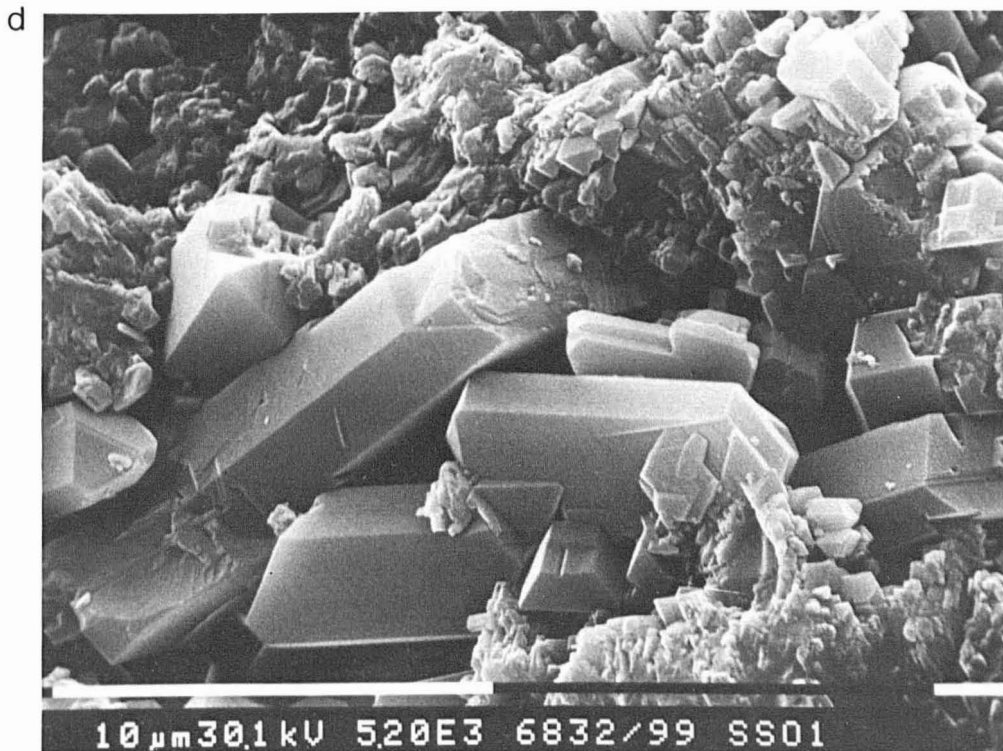
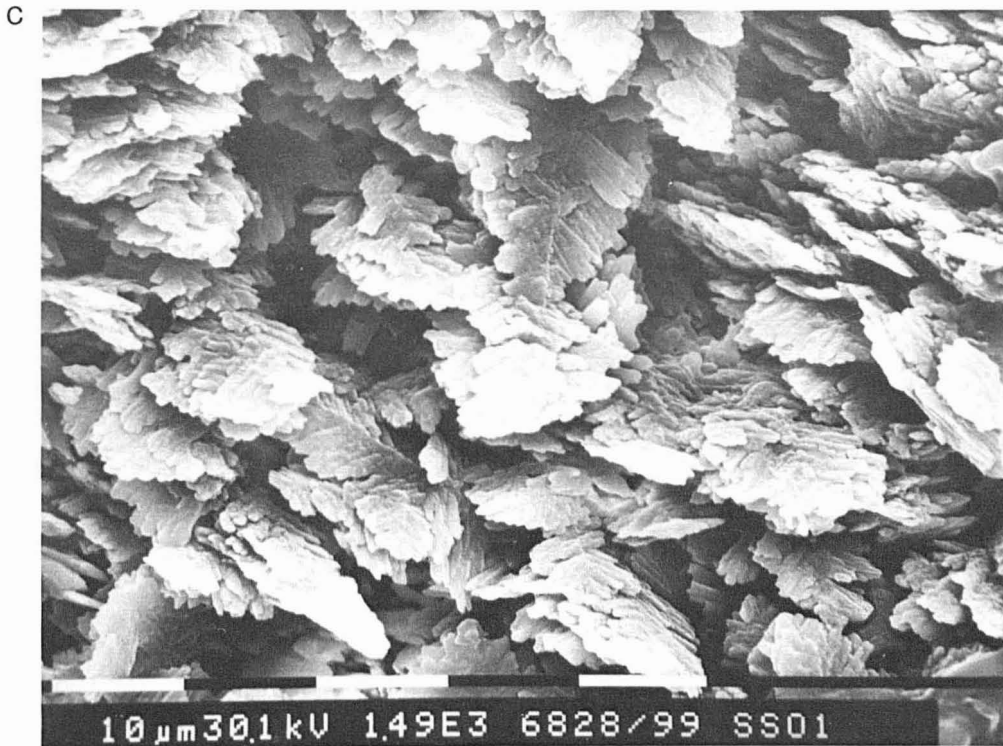


FIGURE 4c.—Leaf-shaped crystals beneath the lateral surface of the broken otolith. Scale bar = 10 μ m.

d.—Calcitic prism crystals beneath the medial surface of the broken irregular lobe. Scale bar = 10 μ m.



FIGURE 4e.—Discontinuous uniform crystal growth forming rings in the broken otolith. Scale bar = 0.1 mm.
f.—Fine and deep (arrowed) increments on the polished and etched otolith surface. Scale bar = 0.1 mm.

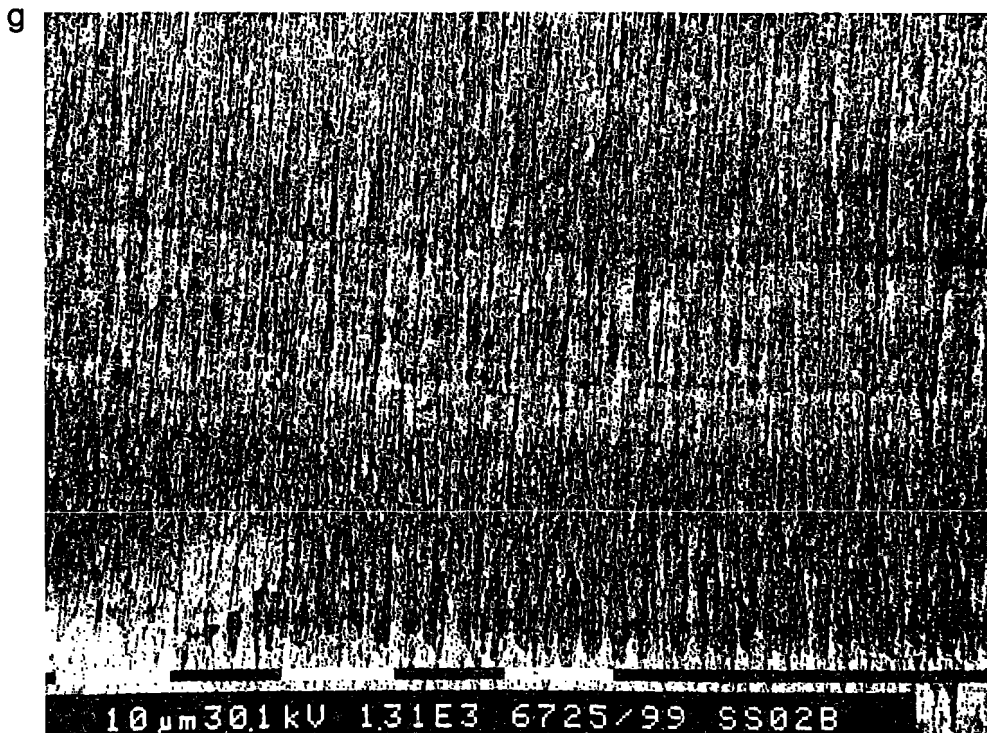


FIGURE 4g.—Fine increments obscured by coarse crystallinity on the polished and etched otolith surface. Scale bar = 10 μ m.

h.—Fine increments (arrowed) found between widely spaced large rings in the otolith cross-section. Magnification = 72 \times .

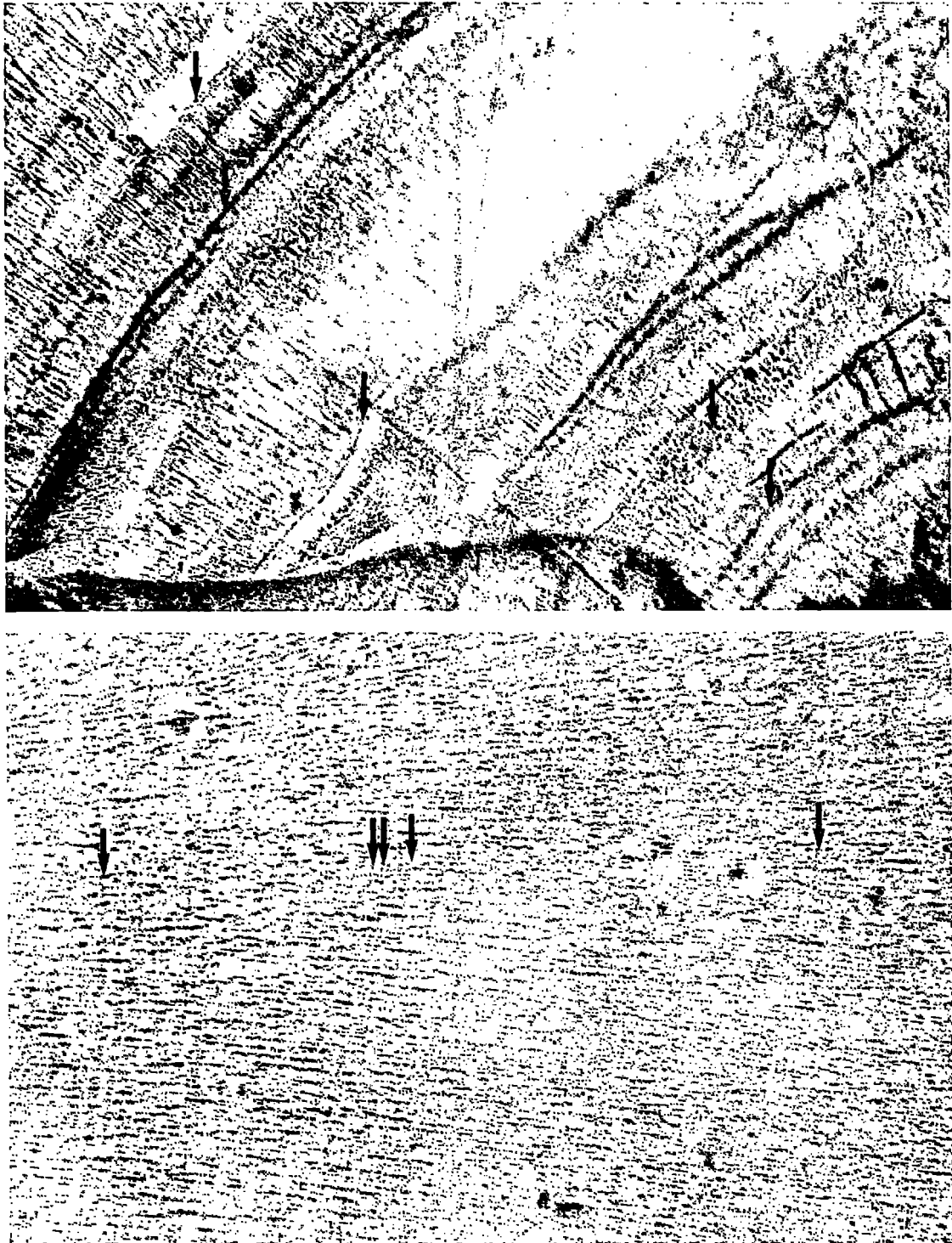


FIGURE 4i.—Variation of increment widths (arrowed) in the otolith cross-section. Magnification = 160 \times .

j.—Cellulose-acetate peel showing the intermittency of fine increment sequences (arrowed), often obscured by a coarse underlying crystallinity. Magnification = 160 \times .

becomes difficult to determine because of the intermittent nature of the growth increments and the variety of width-sizes (Fig. 4i). In large areas of the otolith, increments appear to be absent or indeterminate, with a coarse underlying crystal structure (Fig. 4j) making accurate determination of increment sequences difficult. However, the fine increments of the oreo otolith are 3 to 5 μm wide, which is within the range of daily growth increments described for other species (Jones 1986; Gaudie in press).

Black Oreo Otolith

The black oreo otolith is almost identical to that found in the smooth oreo in overall shape, proportion, structure, topography, surface and internal crystallinity, and increment pattern. Some minor differences do, however, exist.

In the medial sulcus, the prominent knobs found in the smooth oreo otolith are smaller than in the black oreo. On the surface of the sulcus, large leaf-like crystals having various orientations occur (Fig. 5a). Also present in the sulcus are porous, sponge-like crystals adjacent to membranous structures (Fig. 5b). Smooth patches, where crystals appear absent, occur on the lateral surface of the otherwise coarsely crystalline irregular lobe (Fig. 5c). At higher magnification the smooth patches are seen to be smaller growth forms of the larger adjacent crystals.

DISCUSSION

Despite some minor differences in topography and crystallinity, the sagittae of both species are essentially identical. The otoliths are structurally complex with a great variety of crystalline forms. The coarse

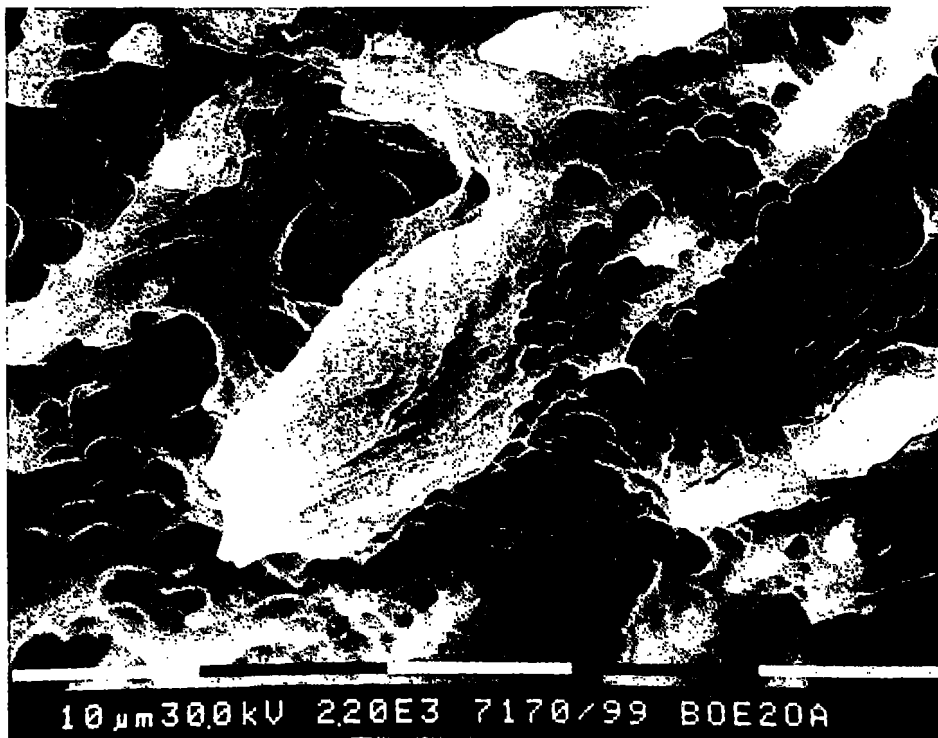


FIGURE 5a.—Split-screen SEM of large leaflike crystals in the black oreo otolith sulcus. Magnification = 356 \times and 979 \times .

b.—Porous, sponge-like crystals in the otolith sulcus. Scale bar = 10 μm .

c.—Smooth patches on the central lateral surface of the otolith. Scale bar = 0.1 mm.

b



c



crystals on the central lateral surface are comparable with those in the oyster shell described as individual laths (Carriker et al. 1980). The leaflike crystals in the sulcus of the black oreo otolith are similar to the chalky crystal forms in the oyster shell (Carriker et al. 1980). Such a variety of crystalline forms is uncommon in teleost otoliths. The low legibility of structures of various kinds in the otolith may reflect this complex crystallinity. However, the complex crystallinity of the mollusc shell is thought to reflect changes in both the external and internal milieu of the organism (Wilbur and Saleuddin 1983). Thus the difficulties of reading the oreo otolith in the conventional sense may be offset by the life history record (albeit difficult to translate) provided by its complex crystallinity.

The broken sections of the otolith reveal the internal structure organization, and development of crystals. Epitaxial crystal growth in the oreo otolith results in columnar, monoclinic crystals of aragonite. However, the presence of calcite-like prisms has not been described for other otoliths. Calcite occurs on the antislural surface of some otoliths apparently by simple crystallization out of the fluid of the endolymphatic sac (Morales-Nin 1985), but calcite has never been described from within an aragonite otolith (Carlstrom 1963). In molluscs, calcite replacement of aragonite results in an orderly alignment of calcite crystals following the alignment of the original aragonite crystals. The disorderly appearance of the calcite-like hexagons in the smooth oreo otolith may be due to a diagenetic transformation of aragonite to calcite with depth. The compensation depth for the aragonite/calcite transformation is about 3,000 m (Fyfe and Bischoff 1965) well beyond the known range of the smooth oreo which has a maximum recorded depth of 1,300 m. However, there may be enough variation in either the kind or amount of stabilizing protein in the smooth oreo otolith to allow crystal changes to occur at shallower depths than 3,000 m.

The complex, and often coarse, crystal structure of the oreo otolith obscures the sequences of increments when they do occur. As a result, large rings observed at low magnification become indistinct at higher magnification when many finer increments appear. The large rings could be assumed to be annual check rings, but the difficulties in differentiating between the fine and large rings create ambivalence in one's interpretation. The finer microscopic growth increments, analogous to daily growth rings, have no uniform width and occur intermittently making accurate counting impossible.

The suitability of an otolith for determining the

age of a fish depends on the pattern of both annual and daily check rings inferred from the structure of the otolith. The hyaline/opaque zones observed in the regular lobe (using transmitted light) had a similar mean width to the concentric ridges found by SEM on the lateral surface. The *t*-statistic we obtained accepts the null hypothesis that no significant difference exists between the two means. Mel'nikov (1981) regarded these opaque/hyaline zones as annual check rings in the otolith of *Allocyttus verrucosus*. However, because no evidence exists for a relationship between the surface ridges and fish age, it is possible that Mel'nikov's (1981) ages are incorrect. Furthermore, the width of the opaque/hyaline zones (0.34 mm) would indicate daily growth increments less than 1 μ m wide. There are no reports in the literature of validated daily growth rings of such small size. In addition, the microscopic growth increments which we have observed in the oreo otolith are 3 to 5 μ m wide, which is a size range commonly observed in other species.

With the techniques available we have been unable to use either annual- or daily-type structures to develop a technique for age estimation for *Pseudocyttus maculatus* and *Allocyttus* sp. The reasons for these difficulties may lie in the crystal morphology of the otoliths which are more complex than any so far described in the literature.

ACKNOWLEDGMENTS

All otoliths were supplied by Peter McMillan (Fisheries Research Centre). All 35 mm photographs were processed by Alan Blacklock (Fisheries Research Centre). SEM photographs were taken at the SEM Unit, Zoology Department, Victoria University of Wellington.

LITERATURE CITED

- CARLSTROM, D.
1963. A crystallographic study of vertebrate otoliths. *Biol. Bull. (Woods Hole)* 125:441-463.
- CARRIKER, M. R., R. E. PALMER, AND R. S. PREZANT.
1980. Functional ultra-morphology of the dissoconch valves of the oyster *Crassostrea virginica*. *Proc. Natl. Shellfish. Assoc.* 70:139-183.
- DEGENS, E. T.
1976. Molecular mechanisms of carbonate, phosphate and silica deposition in the living cell. *Top. Curr. Chem.* 64: 1-112.
- DEGENS, E. T., W. G. DEUSER, AND R. L. HAEDRICH.
1969. Molecular structure and composition of fish otoliths. *Mar. Biol.* 2:105-113.
- FYFE, W. S., AND J. L. BISCHOFF.
1965. The calcite-aragonite problem. In L. C. Pray and R. C. Murray (editors), *Dolomitization and limestone diagenesis*,

- p. 3-13. Symp. Soc. Econ. Minist. Spec. Publ. 13.
- GAULDIE, R. W.
 1987. The fine structure of check rings in the otolith of the New Zealand orange roughy. *NZ J. Mar. Freshwater Res.* 21:267-274.
 In press. A study of otolith daily growth rings in the orange roughy (*Hoplostethus atlanticus*) aimed at resolving problems in age, growth, recruitment and otolith architecture. *NZ Fish. Res. Bull.*
- GAULDIE, R. W., D. DUNLOP, AND J. TSE.
 1986. The remarkable lungfish otolith. *NZ J. Mar. Freshwater Res.* 20:81-92.
- JONES, C.
 1986. Determining age of larval fish with the otolith increment technique. *Fish. Bull.*, U.S. 84:91-103.
- LAST, P. R., E. O. G. SCOTT, AND F. H. TALBOT.
 1983. *Fishes of Tasmania*. Hobart, Tasmanian Fisheries Development Authority.
- MEL'NIKOV, Y. S.
 1981. Size-age composition and growth pattern of *Alloctytus verrucosus* (Oreosomatidae). *Ichthyol. (Engl. transl. Vopr. Ikhtiol.)* 21:178-184.
- MORALES-NIN, B.
 1985. Características de los otolitos cristalinos de *Genypterus capensis*, (Smith, 1847) (Pisces: Ophidiidae). *Invest. Pesq.* 49:379-386.
- MCMILLAN, P. J.
 1985. Black and smooth oreo dories. In J. A. Colman, J. L. McKoy, and G. G. Baird (editors), *Background papers for the 1985 total allowable catch recommendations*. (Report held in the Fisheries Research Centre Library, P.O. Box 297, Wellington, New Zealand.)
- NELSON, J. S.
 1976. *Fishes of the world*. John Wiley and Sons, N.Y., 416 p.
- WATABE, N.
 1983. Shell repair. In A. S. M. Saleuddin and K. M. Wilbur (editors), *The mollusca*, No/4, p 289-316. Acad. Press, N.Y.
- WILBUR, K. M., AND A. S. M. SALEUDDIN.
 1983. Shell formation. In A. S. M. Saleuddin and K. M. Wilbur (editors), *The mollusca*, No/4, p 236-288. Acad. Press, N.Y.